EurJIC European Journal of Inorganic Chemistry
ChemPubSoc Europe

Luminescence

L. Weber,* J. Halama, L. Böhling, A. Brockhinke,* A. Chrostowska,* C. Darrigan, A. Dargelos, H.-G. Stammler, B. Neumann **1–13**

1,3,2-Benzodiazaboroles with 1,3-Pentafluorophenyl and Tetrafluoropyridyl Substituents as Building Blocks in Luminescent Compounds

Keywords: Boron / Diazaboroles / Perfluoroaryls / Photophysics / Luminescence

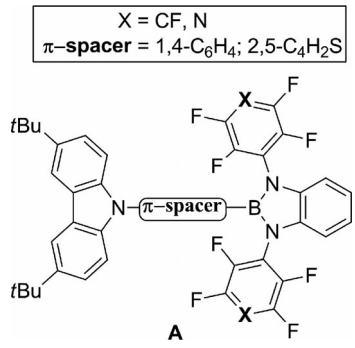

In contrast to π-donating 1,3-diethyl- and 1,3-diphenyl-1,3,2-benzodiazaboroles, derivatives with fluoroaryl substituents at the ring nitrogen atoms are potent π acceptors when connected to a carbazole donor through suitable π-conducting spacers. Thus, molecules of type **A** show low-energy emission bands from charge-transfer (CT) transitions with large Stokes shifts and pronounced solvatochromism.

EurJIC European Journal of Inorganic Chemistry www.eurjic.org FULL PAPER

DOI:10.1002/ejic.201300319

1,3,2-Benzodiazaboroles with 1,3-Pentafluorophenyl and Tetrafluoropyridyl Substituents as Building Blocks in Luminescent Compounds

Lothar Weber,*[a] Johannes Halama,[a] Lena Böhling,[a] Andreas Brockhinke,*[a] Anna Chrostowska,*[b] Clovis Darrigan,[b] Alain Dargelos,[b] Hans-Georg Stammler,[a] and Beate Neumann[a]

Dedicated to Professor Heinrich Nöth on the occasion of his 85th birthday

Keywords: Boron / Diazaboroles / Perfluoroaryls / Photophysics / Luminescence

The reaction of *N*-4′-trimethylsilylphenyl-3,6-di-*tert*-butylcarbazole (**3**) or *N*-5′-trimethylsilylthien-2′-yl-3,6-di-*tert*-butylcarbazole (**4**) with boron tribromide and subsequently with triphenylphosphane afforded the dibromoborylphenylcarbazole–phosphane adduct **5** or its thiophene derivative **6** as colorless solids. These adducts were converted into the new benzodiazaborole derivatives **7** and **8** by treatment with *N*,*N*′-bis(pentafluorophenyl)-*o*-phenylenediamine (**1**) and 2,2,6,6-tetramethylpiperidine in hot toluene (52 or 45% yield). The analogous compounds **9** and **10** were obtained by condensing precursors **5** and **6** with bis(*N*,*N*′-2,3,5,6-tetrafluoropyrid-4-yl)-*o*-phenylenediamine (**2**) in the presence of the piperidine derivative in 35 and 16% yield. Compounds **7**–**10** were characterized by NMR spectroscopy (^{1}H, ^{11}B, ^{13}C, ^{19}F) and mass spectrometry. The molecular structure of **8** was elucidated by X-ray diffraction analysis. The borylated systems show intense blue luminescence upon UV irradiation.

Introduction

Over the last two decades, the development of fluorescent organic compounds for potential application in photonic devices has been a focus of continuing interest. Among the huge number of luminescent species, molecular three-coordinate organoboron compounds and polymers are of emerging importance.[1] Therein, the three-coordinate boron centre usually operates as a π acceptor owing to its vacant p orbital. The dimesitylboryl group ($BMes_2$, Mes = 2,4,6-$Me_3C_6H_2$) is by far the most prominent boron-containing substituent owing to the steric shielding of the unsaturated boron centre by the four *o*-methyl groups. The π-accepting character of the $BMes_2$ unit is similar to those of NO_2 and CN based on UV[2] and cyclic voltammetry data.[3] Conjugated molecules with boryl substituents display very large Stokes shifts and high quantum yields in solution as well as in the solid state, which indicates the lack of close packing as a result of the sterically demanding mesityl groups.[4] In the past decade, the chemistry of 1,3,2-diazaboroles has developed rapidly.[5,6] Some of these compounds are strongly luminescent as solids and in solution.[7] For synthetic reasons, the 1,3-diethyl-1,3,2-benzodiazaborolyl group (1,3-Et_2-1,3,2-$N_2BC_6H_4$) has been frequently used, and compounds with this function are moderately air-stable.[5g,7e–7i] Calculations on 2-arylethynyl-1,3,2-diazaboroles disclosed the localization of the highest occupied molecular orbital (HOMO) on the diazaborole group and led to the suggestion that this group does not function as a π acceptor as originally anticipated but instead behaves as a π-donor substituent.[7i] In line with these observations, it was obvious to study the syntheses and photophysical properties of systems containing two different types of three-coordinate boron centre, which may behave as a π donor on the one end and as a π acceptor on the other end of a rodlike molecule. Thereby, it was found that the π-electron-donating capacity of the 1,3-diethyl-1,3,2-benzodiazaborolyl group towards the $BMes_2$ unit is between that of methoxy and dimethylamino groups.[8] In addition to this, chalcogenodiphenylphosphanyl and alkyldiphenylphosphonium functions were tested for their π-accepting properties towards B/N-heterocycles.[9] Benzodiazaboroles are also potent π-electron donors when ligated to the carbon atoms of *o*-, *m*-, and *p*-*closo*-dicarbadodecaboranes.[10]

[a] Fakultät für Chemie der Universität Bielefeld, 33615 Bielefeld, Germany
E-mail: lothar.weber@uni-bielefeld.de
Homepage: www.Uni-bielefeld.de
[b] IPREM, UMR 5254, Université de Pau et Pays de l'Adour, 64000 Pau, France
E-mail: anna.chrostowska@univ-pau.fr
Supporting information for this article is available on the WWW under http://dx.doi.org/10.1002/ejic.201300319.

At this point, we have been interested in the conditions under which a 1,3,2-benzodiazaborolyl group may undergo an "umpolung" inversion to a π-accepting functionality. Here, it was conceivable to fix a powerful π donor at the opposite end of the organic chain. For this purpose, we selected carbazolyl units, but soon learned that in such species the HOMO and lowest unoccupied molecular orbital (LUMO) are mainly located on the organic part of the molecule, and the benzodiazaborolyl part of the molecule becomes a mere spectator ligand.[7b] As an alternative, the introduction of powerful electron-acceptor substituents at both nitrogen atoms of the B/N-heterocycle seems promising. The present work is focused on the role of 1,3-bis(pentafluorophenyl)- and 1,3-bis(2,3,5,6-tetrafluoropyridin-4-yl)-functionalized 1,3,2-benzodiazaboroles as ligands in *N*-phenyl- and *N*-thienylcarbazoles.

Results and Discussion

Basically, the synthesis of aryl-functionalized 1,3,2-benzodiazaboroles **I** can be accomplished by the two different routes (A and B, Scheme 1).

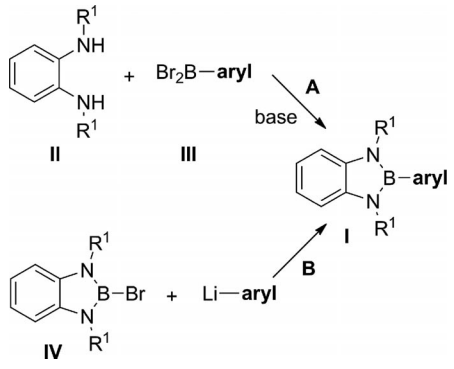

Scheme 1. General synthetic routes to 2-(hetero)aryl-1,3,2-benzodiazaboroles.

Path A is the base-assisted cyclocondensation between an *o*-phenylene diamine **II** and a (hetero)aryldibromoborane **III**, whereas path B involves the nucleophilic substitution of bromide in 2-bromobenzodiazaboroles **IV** by organolithium compounds.[11]

For this work, route A proved to be more efficient and was, thus, preferred over the alternative route B. The required *N*,*N*′-bis(perfluoroaryl)-*o*-phenylenediamines were prepared by reacting *o*-phenylenediamine with 4 equiv. of lithiumbis(trimethylsilyl)amide in tetrahydrofuran (THF) at –78 °C followed by 2 equiv. of hexafluorobenzene[12] or pentafluoropyridine (Scheme 2).

The purification of crude **2** was accomplished by sublimation at 10^{-6} bar and 140 °C, whereby the product was obtained as a pale yellow solid in 67% yield.

The syntheses of (heteroaryl)dibromoboranes **III** were realized by treatment of the appropriate trimethylsilylarenes with boron tribromide. The silylated precursors **3** and **4** resulted from the reaction of freshly prepared organolithiums with chlorotrimethylsilane (TMSCl, Scheme 3).

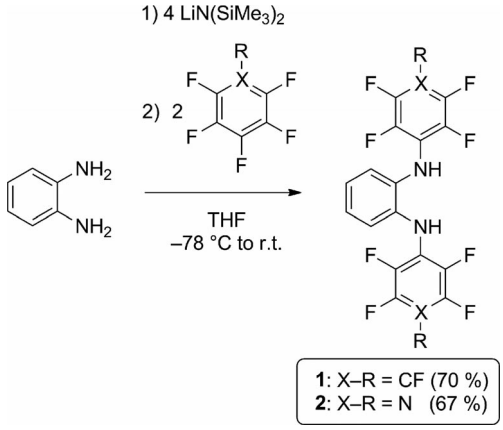

Scheme 2. Syntheses of *o*-phenylenediamines **1** and **2**.

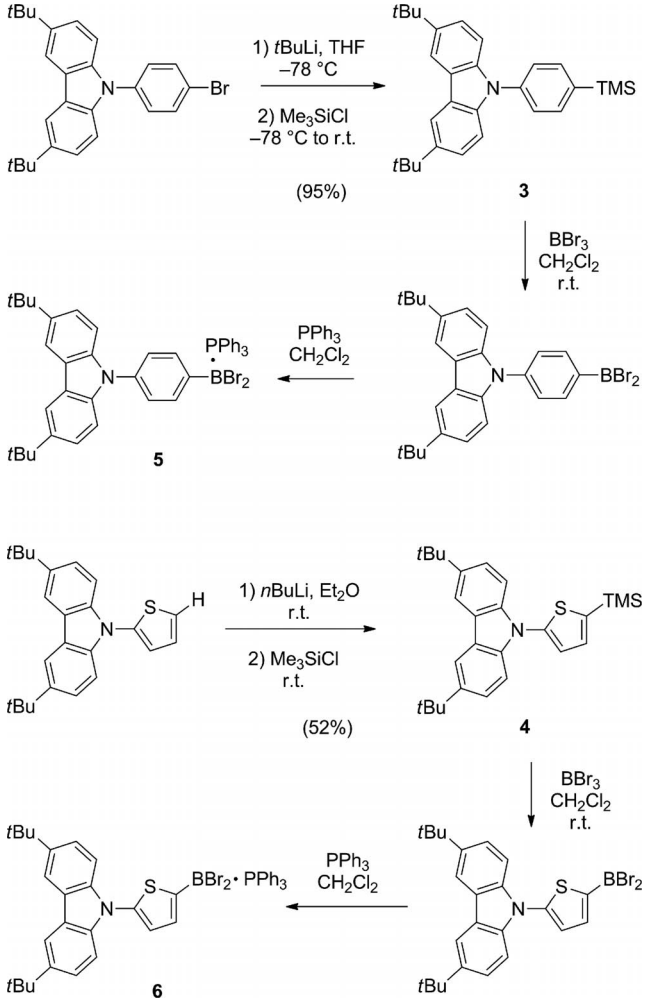

Scheme 3. Syntheses of **5** and **6**.

Compounds **3** and **4** reacted smoothly with an equivalent amount of boron tribromide in dichloromethane within 16 h or 2 h, respectively. As the resulting organodibromoboranes underwent no clean cyclocondensations with the *o*-phenylenediamines **1** and **2**, presumably because of their pronounced Lewis acidity, they were converted into the less reactive triphenylphosphane adducts **5** and **6**. These ad-

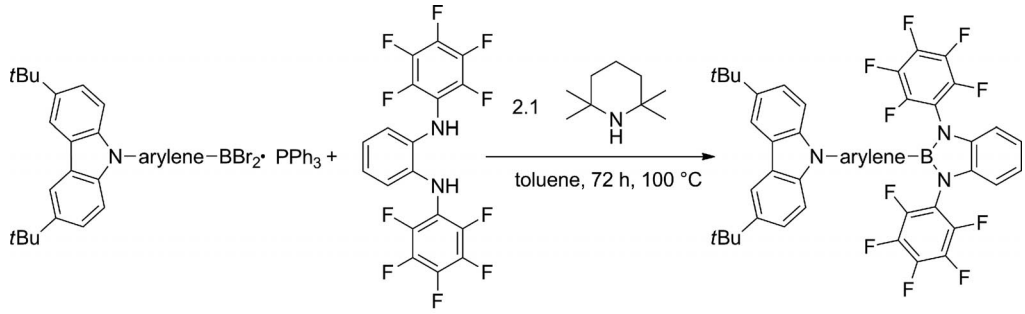

Comp.	Arylene
5, **7**	1,4-C_6H_4
6, **8**	2,5-C_4H_2S

Scheme 4. Syntheses of **7** and **8**.

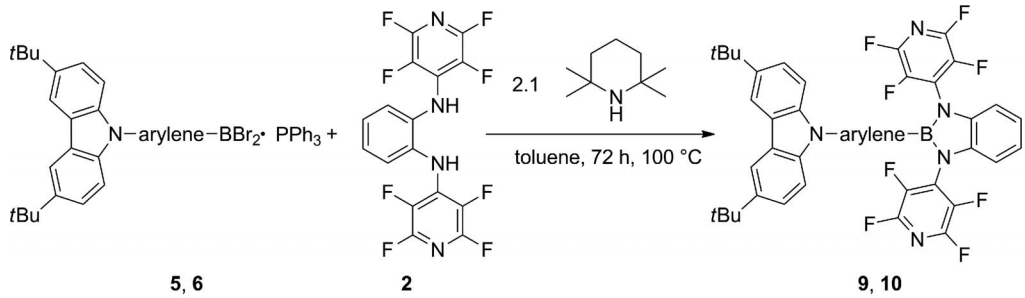

Comp.	Arylene
5, **9**	1,4-C_6H_4
6, **10**	2,5-C_4H_2S

Scheme 5. Syntheses of **9** and **10**.

ducts react with equimolar amounts of phenylenediamine **1** and two equiv. of 2,2,6,6-tetramethylpiperidine in hot toluene (100 °C) in 15 h to afford the new benzodiazaborole derivatives **7** and **8** as pale yellow solids in 52 and 45% yield, respectively. The crude reaction products were separated from triphenylphosphane by sublimation at 100–120 °C (Scheme 4).

Similarly, adducts **5** and **6** were converted to benzodiazaboroles **9** (35%) and **10** (16% yield) by heating them with equimolar amounts of **2** in the presence of 2 equiv. of 2,2,6,6-tetramethylpiperidine (Scheme 5).

The continuous extraction of crude **9** with *n*-hexane over 16 h furnished an analytically pure colorless solid. Crude **10** was extracted with *n*-pentane, and the combined extracts were subsequently stirred with copper(I) iodide to remove excess triphenylphosphane. In this way, pure **10** was obtained as yellow crystals.

For the validation of the utility of 1,3,2-benzodiazaborolyl groups with various aryl- and heteroaryl substituents at the N atoms in luminescent carbazoles, the comparison of **7** and **8** with the non-fluorinated derivatives **11** and **12** was indispensable (Figure 1).

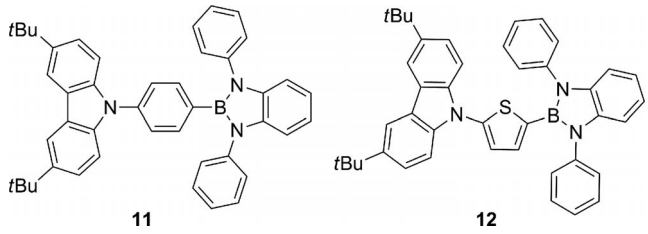

Figure 1. Compounds **11** and **12**.

Compound **12** has been the subject of a recent paper.[7b] The missing link, the 1,3,2-benzodiazaborole derivative **11**, was synthesized from *N*-(4′-bromophenyl)-3,6-di-*tert*-butylcarbazole by lithium/halogen exchange with *n*-butyllithium in diethyl ether at –78 °C and the subsequent quench of the resulting aryllithium species with 2-bromo-1,3-diphenyl-1,3,2-benzodiazaborole. The pure product was obtained as a colorless solid by continuous *n*-hexane extraction over 2 d (yield 63%, Scheme 6).

In contrast to **11**, compounds **7**–**10** are reasonably stable towards moisture and oxygen. They are soluble in $CHCl_3$, CH_2Cl_2, ethers, and aromatic hydrocarbons. In aliphatic hy-

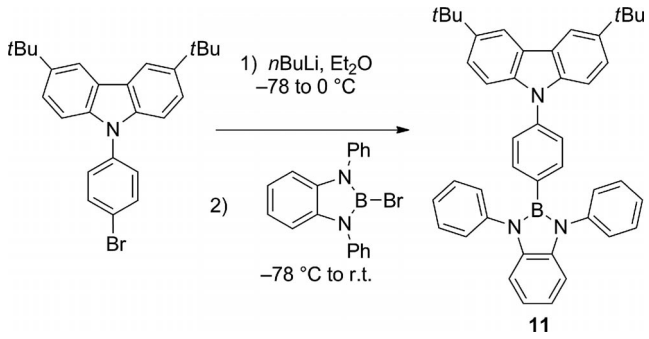

Scheme 6. Synthesis of **11**.

drocarbons, the new benzodiazaborole derivatives are poorly soluble. In the $^{11}B\{^1H\}$NMR spectra broad singlets were observed at δ = 30.7 and 29.9 ppm for of **7** and **9**, respectively, and δ = 27.7 and 28.9 ppm for **8** and **10**, respectively. The incorporation of two N-C_6F_5 substituents as in **7** caused only a slight deshielding of the ^{11}B NMR signal in comparison to that of the non-fluorinated analogue **11** (δ = 29.3 ppm).

X-ray and Computational Structural Analysis of 8

Single crystals of **8** suitable for an X-ray structural study (Table 7) were grown from n-hexane solution at –20 °C. The compound crystallizes in the monoclinic space group $P2_1/c$. The molecule is constructed of three planar rings (Figure 2, Table 1), whereby the central thiophene ring is linked to the benzodiazaborole unit by a single bond B(1)–C(19) [1.530(5) Å], which is slightly shorted in comparison to the B–C bond in **13** [1.557(2) Å], but matches well with that in the 5′-dimesitylboryl-2-N-carbazolylthiophene [**14**, 1.536(3) Å, Figure 3].

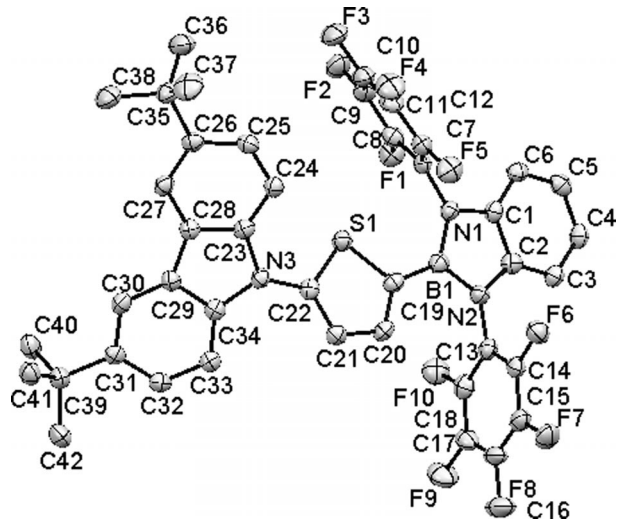

Figure 2. Crystal structure of **8**.

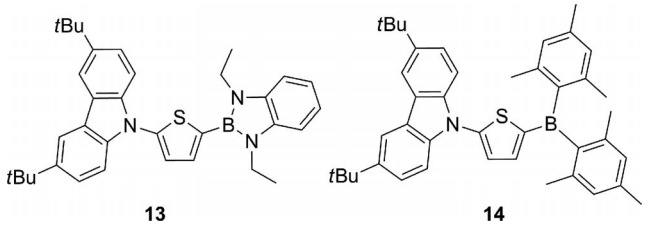

Figure 3. Compounds **13** and **14**.

The thiophene ring is linked in the 2-position to the carbazole fragment by a single N(3)–C(22) bond [1.405(4) Å]. The respective bond lengths in **13** and **14** are 1.405(2) and 1.394(3) Å. The molecule deviates from planarity as evident by the interplanar angles enclosed by the central thiophene ring and the diazaborole plane (10.1°) or the carbazole ring (42°). Although the latter angle is similar to that in **13**

Table 1. Comparison of selected experimental and [CAM-B3LYP/6-311G(d,p)] calculated bond lengths [Å] and angles [°] for **8**.

Bond	Experimental	CAM-B3LYP	Angle	Experimental	CAM-B3LYP
B(1)–N(1)	1.440(4)	1.4397	N(1)–B(1)–N(2)	104.5(3)	105.41
B(1)–N(2)	1.441(4)	1.4367	B(1)–N(1)–C(1)	109.5(2)	108.79
N(1)–C(1)	1.421(4)	1.4072	B(1)–N(1)–C(7)	127.8(3)	128.11
N(2)–C(2)	1.411(4)	1.4070	B(1)–N(2)–C(2)	109.7(2)	108.90
N(1)–C(7)	1.415(4)	1.4053	B(1)–N(2)–C(13)	126.9(2)	128.12
N(2)–C(13)	1.417(4)	1.4045	N(1)–C(1)–C(2)	107.9(2)	108.45
C(1)–C(2)	1.397(4)	1.3978	N(2)–C(2)–C(1)	108.4(2)	108.44
B(1)–C(19)	1.530(5)	1.5394	N(1)–B(1)–C(19)	128.6(3)	127.66
S(1)–C(19)	1.729(3)	1.7325	N(2)–B(1)–C(19)	126.8(3)	126.89
S(1)–C(22)	1.721(3)	1.7373	B(1)–C(19)–S(1)	120.4(2)	122.32
C(19)–C(20)	1.370(4)	1.3701	B(1)–C(19)–C(20)	130.6(3)	127.48
C(20)–C(21)	1.407(4)	1.4169	C(19)–S(1)–C(22)	92.6(1)	92.14
C(21)–C(22)	1.361(4)	1.3619	S(1)–C(22)–C(21)	111.6(2)	111.17
N(3)–C(22)	1.405(4)	1.3929	C(20)–C(21)–C(22)	111.7(3)	112.44
N(3)–C(23)	1.416(4)	1.3980	S(1)–C(19)–C(20)	108.9(2)	109.95
N(3)–C(34)	1.412(4)	1.3972	C(19)–C(20)–C(21)	115.3(3)	114.23
C(23)–C(28)	1.397(4)	1.4024	S(1)–C(22)–N(3)	120.0(2)	120.70
C(28)–C(29)	1.457(4)	1.4491	C(21)–C(22)–N(3)	128.3(3)	128.12
C(29)–C(34)	1.405(4)	1.4026	C(23)–N(3)–C(34)	107.8(2)	108.25
			C(22)–N(3)–C(23)	125.1(2)	125.58

(41.4°), the diazaborole ring is clearly more twisted into the thiophene plane in **8** than in **13** (34.7°), which points to more π interaction between the better π-accepting fluorinated borole in comparison to the *N*,*N*′-dialkyl derivative in **13**. The bond lengths and angles within the benzodiazaborole part are as usual. The bond lengths within the thiophene building block [S(1)–C(19) 1.729(3) Å, S(1)–C(22) 1.721(3) Å] C(19)–C(20) 1.370(4) Å, C(20)–C(21) 1.407(4) Å, and C(21)–C(22) 1.361(4) Å] are close to those in **13** [1.735(1), 1.735(1), 1.373(2), 1.416(2), and 1.364(2) Å]. As also observed in **13**, the exocyclic angles B(1)–C(19)–S(1) [120.4(2)°] and B(1)–C(19)–C(20) [130.6(3)°] differ significantly. Similar observations were made with angles S(1)–C(22)–N(3) [120.0(2)°] and C(21)–C(22)–N(3) [128.3(3)°].

In Table 1, the [CAM-B3LYP/6-311G(d,p)] calculated geometrical parameters for **8** are compared with the experimental results (see Supporting Information for the calculated geometrical parameters of **7**–**11**).

In comparison to the experimentally determined geometrical parameters of the crystal structure of **8**, the theoretically derived gas-phase ones agree nicely and show that the CAM-B3LYP method associated with 6-311G(d,p) is well suited to the prediction and evaluation of the geometries of the studied molecules.

UV/Vis and Luminescence Spectra/DFT Calculations

Selected photophysical data for **7**–**10** are compiled in Table 2; all compounds exhibit intense blue luminescence under UV irradiation. Compounds **11** and **12** featuring 1,3-diphenyl-1,3,2-benzodiazaborole groups and the carbazoles **15** and **16** are also considered for comparison.

The UV/Vis spectra of **7**–**10** (in cyclohexane) show intense bands at λ = 294–296 nm (ε = 20800–33400 L mol^{-1} cm^{-1}) in addition to a less intense band at λ = 340–344 nm (ε = 11600–17000 L mol^{-1} cm^{-1}). In **11**, for comparison, absorption bands at λ = 297 (ε = 11900 L mol^{-1} cm^{-1}) and 344 nm (ε = 4400 L mol^{-1} cm^{-1}) were measured and are identical to those in the fluorinated derivatives as well as in carbazoles **15** and **16** (Figure 4).

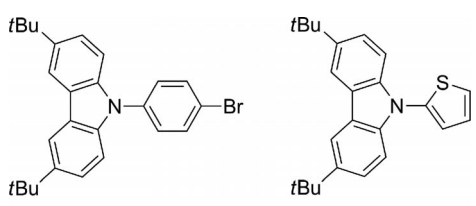

15 **16**

Figure 4. Carbazoles **15** and **16**.

The positions of these absorptions in THF and CH_2Cl_2 solutions are virtually the same. The absence of solvatochromism points to a minor change of dipole moment of these compounds during the absorption. This observation is in accord with local transitions without the participation of the benzodiazaborolyl unit. In the luminescence spectrum of **7** in cyclohexane, there is a strong band at λ = 358 nm (Stokes shift 1200 cm^{-1}), which in the more polar solvents THF or CH_2Cl_2 is redshifted to λ = 395 (Stokes shift 4000 cm^{-1}) and 407 nm (Stokes shift 4800 cm^{-1}), respectively. These Stokes shifts as well as the solvatochromism are consistent with an excited state of increased polarity as the result of an intramolecular charge transfer (CT). In contrast to this, the non-fluorinated analogue **11** shows an emission at λ = 354 nm in cyclohexane (Stokes shift 600 cm^{-1}) with virtually no solvatochromism (THF: λ = 355 nm, Stokes shift 900 cm^{-1}; CH_2Cl_2: λ = 358 nm, Stokes shift 1200 cm^{-1}). A similar situation was observed with *p*-bromophenylcarbazole **15** (λ = 350–255 nm; Stokes shift 500–900 cm^{-1}) These differences may be explained by the nature of the transitions, which in the case of **11** and **15** are local transitions within the carbazole part, whereas a CT from the carbazole to the benzodiazaborole occurs in **7**. The formal replacement of the phenylene spacer in **7** by the thiophene-2,5-diyl bridge in **8** did not change the absorptions in the UV/Vis spectra significantly (cyclohexane: λ = 295, 340 nm; THF: λ = 294, 340 nm; CH_2Cl_2: λ = 294, 340 nm). Here, solvatochromism is again virtually absent. In the luminescence spectrum of **8**, however, the emission band in *c*-C_6H_{12} is markedly redshifted to λ = 394 nm (Stokes shift 4000 cm^{-1}). This band is more sensitive to the polarity of the solvent and is redshifted to λ = 405 nm (Stokes shift 4900 cm^{-1}) in THF and λ = 411 nm (Stokes shift 5300 cm^{-1}) in CH_2Cl_2.

In the benzodiazaborole derivatives **9** and **10**, the exchange of both *N*-pentafluorophenyl substituents by two 2,3,5,6-tetrafluoro-4-pyridyl groups had no significant influence on the low-energy and solvent-insensitive absorptions in the UV/Vis spectra. However, the luminescence spectra are somewhat different and merit special comments. In *c*-C_6H_{12}, the phenylene-bridged species **9** displays a single emission band at λ = 377 nm (Stokes shift 2900 cm^{-1}), which is bathochromically shifted in comparison to that of the C_6F_5 analogue **7**. However, the two emissions are recorded at λ = 354 and 418 nm in THF and λ = 356 and 414 nm in CH_2Cl_2. The Stokes shifts for the low-energy emissions, which correspond to intramolecular charge-transfer transitions, are 5300 and 5600 cm^{-1}.

In derivative **10**, which features the thiophene-based linker, two emissions are also observed in cyclohexane at λ = 357 nm and 410 nm. They are redshifted to λ = 366 and 428 nm in THF and λ = 367 and 431 nm in CH_2Cl_2. The corresponding Stokes shifts are 5000, 6200, and 6300 cm^{-1}. To reach a deeper understanding of this phenomenon, the luminescence spectra of **9** and **10** were recorded in a number of solvents of different orientation polarization (Figure 5, Table 3).

From inspection of the emission bands of **10** in various solvents, it is clear that the band at $\lambda \approx$ 360 nm increased in intensity with increasing polarity of the solvent, accompanied by a weak solvatochromism. Usually, the CT emissions of known benzodiazaboroles are quenched in acetonitrile because of adduct formation. Here, however, for the first time, the CT band at λ = 447 nm is clearly more prominent the high-energy band at λ = 381 nm.

Table 2. Selected photophysical data of **7**–**12**, **15**, and **16**.

	Solvent	$\lambda_{max,abs}$ [nm]	$\tilde{\nu}_{max,abs}$ [cm^{-1}]	ε [L mol^{-1} cm^{-1}]	$\lambda_{max,em}$ [nm]	$\tilde{\nu}_{max,em}$ [cm^{-1}]	Stokes shift [cm^{-1}]	Φ_F [%]
	c-C_6H_{12}	296	33800	26600	358	27900	1200	79
		344	29100	17000				
7	THF	297	33700	18200	395	25100	4000	15
		344	29100	8300				
	CH_2Cl_2	297	33700	25400	407	24300	4800	26
		344	29100	10000				
	c-C_6H_{12}	294	34000	23700	394	25400	4000	14
		340	29400	15600				
8	THF	294	34000	24000	405	24500	4900	9
		340	29400	16300				
	CH_2Cl_2	294	34000	17300	411	24100	5300	18
		340	29400	12000				
	c-C_6H_{12}	295	33900	20800	377	26200	2900	47
		344	29100	11600				
9	THF	296	33800	15300	354	23600	5300	7
		344	29100	6400	418			
	CH_2Cl_2	296	33800	25400	356	23900	5600	2
		344	29100	10400	414			
	c-C_6H_{12}	295	33900	33400	357	24400	5000	16
		340	29400	11600	410			
10	THF	295	33900	36500	366	23200	6200	3
		340	29400	15600	428			
	CH_2Cl_2	295	33900	34000	367	23100	6300	2
		341	29300	15900	431			
	c-C_6H_{12}	297	33700	11900	353	28300	600	79
		344	29100	4400				
11	THF	297	33700	21500	355	28100	900	21
		345	29000	8400				
	CH_2Cl_2	297	33700	14700	358	27800	1200	38
		345	29000	4900				
	c-C_6H_{12}	296	33800	22600	386	25500	5200	13
		328	30500	9900				
12	THF	296	33800	28600	388	25300	5000	14
		330	30300	11200				
	CH_2Cl_2	297	33700	15400	396	25000	5300	18
		330	30300	10700				
	c-C_6H_{12}	297	33700	18700	350	28600	500	11
		344	29100	3600				
15	THF	297	33700	23000	353	28300	800	12
		344	29100	4100				
	CH_2Cl_2	297	33700	25100	355	28200	900	8
		344	29100	4400				
	c-C_6H_{12}	296	33800	26100	356	28100	1400	3
		339	29500	3600				
16	THF	296	33800	20300	364	27300	2200	2
		339	29500	3200				
	CH_2Cl_2	296	33800	24900	370	26900	2400	2
		341	29300	3900				

In the luminescence spectra of **9**, a more pronounced solvatochromism in addition to high-energy emissions at λ = 354 and 356 nm were observed in THF and CH_2Cl_2. In contrast, in acetonitrile only one emission at λ = 360 nm was recorded. The high-energy emissions in **9** and **10** appeared in the region in which the emissions of carbazoles **15** and **16** (λ = 350–355 nm and 356–370 nm) occurred.

The fluorescence at λ = 355 nm of carbazole **15** in CH_2Cl_2 (Table 4) has a lifetime of τ = 3.67 ns, which reflects a local transition within the carbazole. The high-energy emission band of **9** in CH_2Cl_2 at λ = 356 nm has a lifetime of τ = 3.69 ns and, thus, belongs to the same local transition. The single emission of **9** in cyclohexane at λ = 376 nm and the band at λ = 414 nm in the emission spectrum of **9** in CH_2Cl_2 have similar lifetimes (τ = 2.51 and 2.45 ns, respectively) and are assigned to the same intramolecular CT emission from the benzodiazaborole back to the carbazole. It is further remarkable that the CT-emission bands of **9** in THF and CH_2Cl_2 have long tails in comparison to those in the other solvents under investigation. One possible

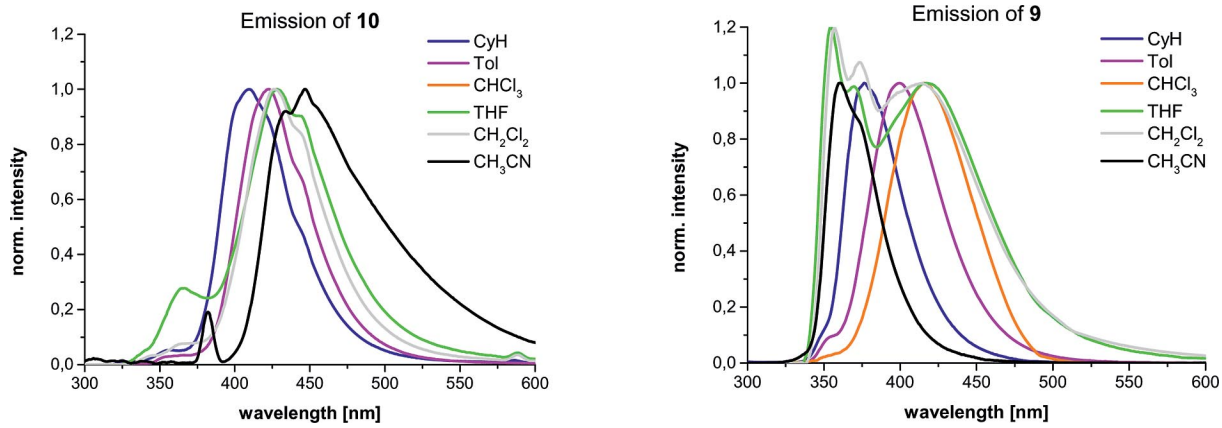

Figure 5. Emissions of **9** and **10** in solvents of increasing orientation polarization.

Table 3. Emission maxima [nm] of **9** and **10** in solvents of increasing orientation polarity.

	c-C_6H_{12}	Toluene	$CHCl_3$	THF	CH_2Cl_2	CH_3CN
9	377	400	417	354, 420	356, 414	360
10	357, 410	358, 423	365, 426	366, 428	367, 431	381, 447

Table 4. Fluorescence lifetimes of **9** and **15**.

	Solvent	Wavelength [nm]	Lifetime [ns]
9	CyH	376	2.51
	CH_2Cl_2	356	3.69
	CH_2Cl_2	414	2.45
15	CH_2Cl_2	355	3.67

explanation for this could be a weak transition from the benzodiazaborole ring to the electron-withdrawing tetrafluoropyridyl substituents. For example, in the fluorescence spectrum of 2-bromo-1,3-bis(tetrafluoropyridyl)-1,3,2-benzodiazaborole, emissions at λ = 477 nm in c-C_6H_{12} and λ = 502 nm in CH_2Cl_2 of low intensity ($\Phi_F \approx 1\%$) were observed. In addition, a fluorescence spectrum of solid **9** was measured by means of the integrating-sphere method, whereby an emission maximum appeared at λ = 386 nm. The emission band had a large tail towards lower energies and a quantum yield (Φ_F) of 5%. The band is slightly redshifted when compared with that of **9** in cyclohexane solution. Despite the assignment of the respective emission bands to local and charge-transfer transitions the occurrence of the additional maxima in polar solvents such as THF or CH_2Cl_2 deserves further explanation. Therefore, emission spectra were recorded at varying concentrations. However, no significant changes or new bands were observed, and the formation of excimers or packing effects in the solid can be excluded. Solutions of **9** in methanol, 2-propanol, pyridine, triethylamine, and dimethylsulfide, which usually react with a diazaborole, only show the high-energy emission at $\lambda \approx 355$ nm, which clearly agrees with the quench of the CT emission. Finally, a toluene solution of **9** was combined in portions with CH_2Cl_2. At a toluene/dichloromethane ration of 2:1 the emission band shifts slightly to larger wavelengths. Thus, a Lewis acid–base adduct of **9** with CH_2Cl_2 seems unlikely. The appearance of the two emissions of **9** in pure CH_2Cl_2 or THF are presumably because the polarity of the solvent cage stabilizes a geometry in which CT transitions from the carbazole to the benzodiazaborole and from the B/N-heterocycle to the tetrafluoropyridine are observable in addition to the local π–π* transition in the *N*-phenylcarbazole part.

The calculated absorption maxima from time-dependent DFT (TD-DFT) computations on **7**–**11** and the dipole moment of ground and first excited states are displayed in Table 5. The most intense absorption is calculated for **11** at 281.1 nm and corresponds to the energy of the HOMO–LUMO+1 transition. This band is observed in the UV/Vis spectrum as the most intense band at λ = 297 nm, and the calculated small ground state dipole moment μ_g (0.655 D) explains the observed absence of solvatochromism for this compound. For **7**, the most intense absorption corresponding to the HOMO–LUMO transition is calculated at 289.7 nm for the experimentally observed λ = 296 nm, and the change of the ground state dipole moment upon excitation is not significant (μ_g = 1.043 D; μ_{exc} = 1.417 D). For **8**, **9**, and **10**, this lowest-energy absorption is calculated at the highest wavelength (302.7, 298.2, and 310.0 nm, respectively) if compared to **7** or **11**. In comparison with the experimental values, the measured absorption values for **7** and **11** (in c-C_6H_{12}) are redshifted by 6.3 and 15.9 nm, respectively, whereas the calculated absorption maximum of **8**, **9**, and **10** are blueshifted by 8.7, 3.2, and 15.0 nm, respectively. For these three molecules, the calculated ground state dipole moments μ_g are small (in order of increasing strength: **8** 1.005 D, **10** 1.541 D, **9** 1.567 D), but these dipole moments change significantly upon excitation of the ground state to the first excited state in **9** (9.593 D), **8** (9.894 D), and **10** (10.756 D) and reflect a significant charge transfer upon excitation.

These values are obviously underestimated and deviate significantly from the experimentally determined transition dipole moments by means of the Lippert–Mataga method (**7** 21.4 D. **8** 14.7 D, **9** 19.9 D, **10** 20.7 D).[13] The calculated dipole moments are derived in the gas phase with solvation effect neglected, which may cause these deviations.

Table 5. Comparison of [CAM-B3LYP/6-311+G(d,p)] calculated data for optimized geometries of **7**–**11** and observed UV absorption maxima (in c-C_6H_{12}) [nm]; calculated values of dipole moment of ground (μ_g) and first excited (μ_{exc}) states [D].

Compound.	λ_{max} (calcd.)	Oscillator strength (f)	λ_{max} (exp)	$\Delta\lambda_{max}$ (calc – exp)	Ground state dipole moment (μ_g)	Excited state dipole moment (μ_{exc})	Transition dipole moment (exp)
7	289.7	0.27	296	–6.3	1.043	1.417	21.4
8	302.7	0.29	294	8.7	1.005	9.894	14.7
9	298.2	0.40	295	3.2	1.567	9.593	19.9
10	310.0	0.23	295	15.0	1.541	10.756	20.7
11	281.1	0.50	297	–15.9	0.655	2.519	–

The [CAM-B3LYP/6-311G(d,p)] calculated MO energies ε^{KS} (LUMO+2, LUMO+1, LUMO, HOMO, HOMO–1, HOMO–2) of **7**–**11** as well as the HOMO–LUMO gap (Δ_{H-L}) are displayed in Table 6. The LUMOs of **7**, **8**, and **11** are located at the vacant $2p_z$ orbital of the B atom with contributions from π* of the arylene unit (phenyl in **7** and **11** or thiophene in **8**), whereas the LUMOs of **9** and **10** are mainly located at two 2,3,5,6-tetrafluoro-4-pyridyl groups.

Table 6. [CAM-B3LYP/6-311G(d,p)] calculated MO energies ε^{KS} (LUMO+2, LUMO+1, LUMO, HOMO, HOMO–1, HOMO–2), HOMO–LUMO gap of **7**, **8**, **9**, **10**, and **11**. Contour values are plotted at ±0.04 e bohr^3). Element (color): H (white), B (light pink), C (gray), N (dark blue), F (light blue), S (yellow); Ph: phenyl; th: thiophene; crb: carbazole.

	7	**8**	**9**	**10**	**11**
LUMO+2	+0.046 π*(*Ph*) 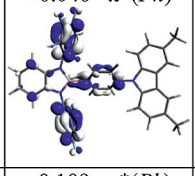	+0.010 π*(*Ph*) 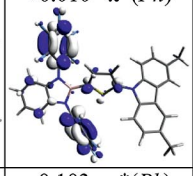	–0.183 $2p_z$*–π*(*Ph*) 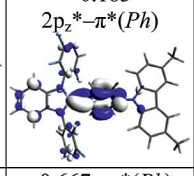	–0.322 $2p_z$*–π*(*th*) 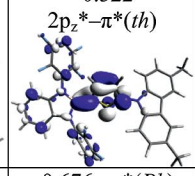	+0.601 π*(*Ph*) 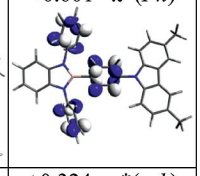
LUMO+1	–0.109 π*(*Ph*) 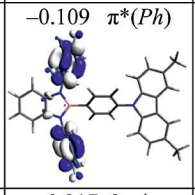	–0.103 π*(*Ph*) 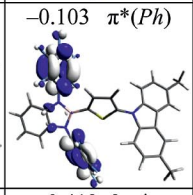	–0.667 π*(*Ph*) 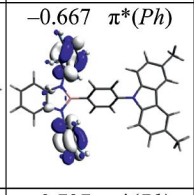	–0.676 π*(*Ph*) 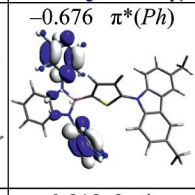	+0.324 π*(*crb*) 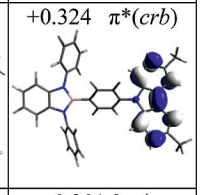
LUMO	–0.217 $2p_z$*–π*(*Ph*) 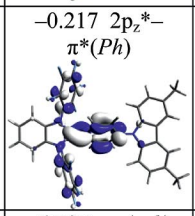	–0.412 $2p_z$*–π*(*Ph*) 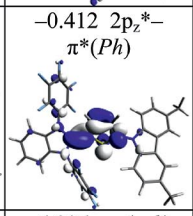	–0.737 π*(*Ph*) 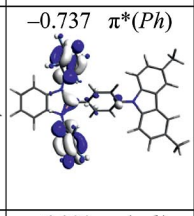	–0.818 $2p_z$*–π*(*Ph*) 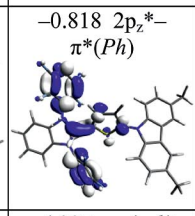	+0.201 $2p_z$*–π*(*Ph*) 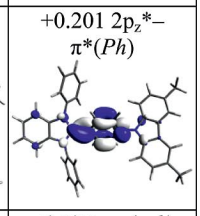
HOMO	–6.787 π_1(*crb*) 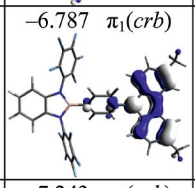	–6.896 π_1(*crb*) 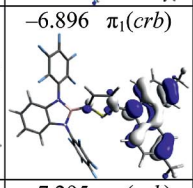	–6.823 π_1(*crb*) 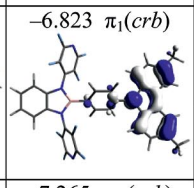	–6.937 π_1(*crb*) 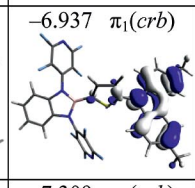	–6.595 π_1(*crb*) 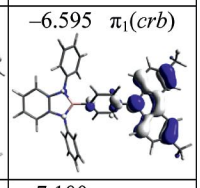
HOMO–1	–7.243 π_2(*crb*) 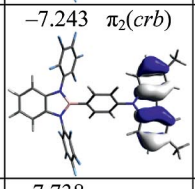	–7.295 π_2(*crb*) 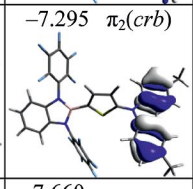	–7.265 π_2(*crb*) 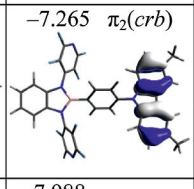	–7.309 π_2(*crb*) 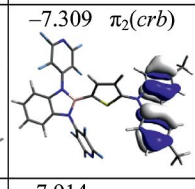	–7.100 π_3–π_{NBN} 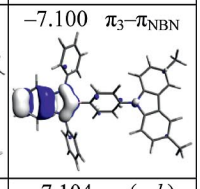
HOMO–2	–7.738 π_3–π_{NBN} 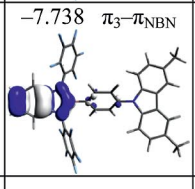	–7.660 π_3–π_{NBN} 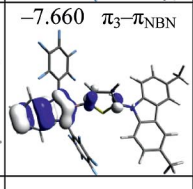	–7.988 π_3–π_{NBN} 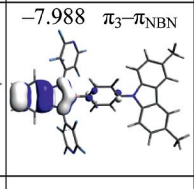	–7.914 π_3–π_{NBN} 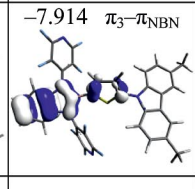	–7.104 π_2(*crb*) 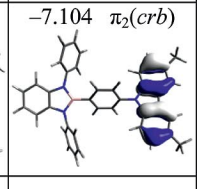
Δ_{H-L} (eV; nm)	6.570; 188.7	6.484; 191.2	6.086; 203.7	6.119; 202.6	6.796; 182.4

The HOMOs in the five molecules correspond to π_1(crb) and are located on the carbazole part, whereas the HOMO–1s are linked with the π_2(crb) in **7**, **8**, **9**, and **10**. For **11**, the latter is located at the benzodiazaborole part. HOMO–2 involves the benzodiazaborole group in **7**–**10** or the carbazole group (π_2) in **11**. The replacement of the phenyl substituents on the benzodiazaborole nitrogen atoms in **11** by the pentafluorophenyls in **7** leads to a significant stabilization of all ionization energies. This effect is also found from **11** to **9**, in which the phenyl groups are replaced by tetrafluoropyridyls. In contrast, the replacement of the spacer from phenyl in **7** or **9** to the thiophene in **8** or **10**, respectively, is not significant and the HOMO is only very slightly stabilized in **8** (0.109 eV) and in **10** (0.114 eV) in comparison to those of **7** and **9**.

Conclusions

1,3,2-Benzodiazaboroles are ambiguous functionalities when attached to extended organic π-conjugated scaffolds and their properties depend on the nature of the substituents at the nitrogen atoms in the 1- and 3-position. With ethyl and phenyl substituents, these heterocycles mainly appear as π donors in push–pull molecules, whereas with electron-withdrawing groups such as pentafluorophenyl or tetrafluoropyridyl at the N atoms of the benzodiazaborolyl moieties, they experience an "umpolung" transition into π acceptors when linked to carbazole donors through 1,4-phenylene or 2,5-thiophenediyl spacers. In keeping with this, the fluorescence spectra of **7**–**10** show low-energy emission bands resulting from CT transitions with large Stokes shifts and pronounced solvatochromism.

Experimental Section

General: All manipulations were performed under an atmosphere of dry, oxygen-free argon by using Schlenk techniques. All solvents were dried by standard methods and freshly distilled prior to use. *N*,*N*′-Bis(pentafluorophenyl)-*o*-phenylene diamine (**1**)[12] and *N*-(4-bromophenyl)-3,6-di-*tert*-butylcarbazole[14] were prepared according to literature methods.

Hexafluorobenzene, pentafluoropyridine, hexamethyldisilazane, boron tribromide, triphenylphosphane, chlorotrimethylsilane, and *n*-butyllithium (1.6 M in *n*-hexane) were purchased commercially. NMR spectra were recorded at room temperature with (a) a Bruker Avance III 300 (^{1}H: 300, ^{11}B: 96, ^{13}C: 75, ^{19}F: 282 MHz) and (b) a Bruker Avance III 500 spectrometer (^{1}H: 500, ^{11}B: 160, ^{13}C: 125, ^{19}F: 470, ^{31}P: 202 MHz) with $SiMe_4$ (^{1}H, ^{13}C), $BF_3{\cdot}OEt_2$ (^{11}B), $CFCl_3$ (^{19}F), and 85% H_3PO_4 (^{31}P) as external standards. Mass spectra were obtained with a VG autospec sector field mass spectrometer (Micromass).

Photophysical Measurements: For all solution-state measurements, samples were placed in quartz cuvettes of 10× 10 mm (Hellma type 111-QS, suprasil, optical precision). Cyclohexane was used as received from commercial sources (p. a. quality), and the other solvents were dried by standard methods prior to use. The concentrations varied from 20 to 70 μM according to their optical density. Solid sample were prepared by vacuum sublimation on quartz plates (35× 10× 1 mm) by using standard Schlenk equipment and conditions. Absorption was measured with a UV/Vis double-beam spectrometer (Shimadzu UV-2550) with the solvent as a reference.

The output of a continuous Xe lamp (75 W, LOT Oriel) was wavelength-separated by a first monochromator (Spectra Pro ARC-175, 1800 lines/mm grating, blaze 250 nm) and then used to irradiate a sample. The fluorescence was collected by mirror optics at right angles and imaged on the entrance slit of a second spectrometer; astigmatism was corrected at the same time. The signal was detected by a back-thinned CCD camera (RoperScientific, 1024× 256 pixels) in the exit plane of the spectrometer. The resulting images were spatially and spectrally resolved. In the next step, an averaged fluorescence spectrum was calculated from the raw images and stored in the computer. This process was repeated for different excitation wavelengths. The result is a two-dimensional fluorescence pattern with the excitation wavelength on the *y* axis and the emission wavelength on the *x* axis. The wavelength range is λ_{ex} = 230–430 nm (in 1 nm increments) for the UV light and λ_{em} = 305–894 nm for the detector. The time to acquire a complete excitation emission spectrum (EES) is typically less than 15 min. Post-processing of the EES includes subtraction of the dark current background, conversion of pixel to wavelength scales, and multiplication with a reference file to take the varying lamp intensity as well as grating and detection efficiency into account. The quantum yields were determined against *p*-bis(5-phenyl-2-oxazolyl)benzene (POPOP, Φ_F = 0.93) as the standard.

The solid-state fluorescence was measured by addition of an integrating sphere (Labsphere, coated with Spectralon, Ø = 12.5 cm) to the existing experimental setup. At the exit slit of the first monochromator, the exciting light was transferred into a quartz fiber (LOT Oriel, LLB592). It passed a condenser lens and illuminated a 1 cm^2 area on the sample in the centre of the sphere. The emission and exciting light was imaged by a second quartz fiber on the entrance slit of the detection monochromator. The optics for correction of astigmatism was passed by the light in this way.

The luminescence lifetimes of **9** and **15** were measured with a time-correlated single-photon counting apparatus (TCSPC, Horiba Jobin Yvon FluoroHub, light source: Nano-LED280, detector: Photomultiplier TBX).

Computational Details: All calculations were performed by using the Gaussian 09[15] program package with the 6-311G(d,p) basis set, except for the calculations of UV absorptions for which the 6-311+G(d,p) basis set was applied. DFT has been shown to predict various molecular properties successfully.[16] All geometry optimizations were performed with the CAM-B3LYP[17] functional and were followed by frequency calculations to verify that the stationary points obtained are true energy minima. The TD-DFT[18] approach provides a first principals method for the calculation of excitation energies within a density functional context taking into account the low-lying ion calculated by ΔSCF method.

***N*,*N*′-Bis(tetrafluoro-4-pyridyl)-*o*-phenylenediamine (2):** Similarly to ref.[12], a cold THF solution (150 mL, –78 °C) of *o*-phenylenediamine (5.0 g, 46 mmol) was lithiated and combined with pentafluoropyridine (15.59 g, 10.1 mL, 92.2 mmol). After work-up, the brown solid residue was sublimed at 1× 10^{-1} bar and 140 °C. Crude **2** was collected as a yellow sublimate and was subsequently purified by crystallization from benzene (250 mL) to afford 12.5 g of analytically pure **2** as a pale yellow solid (67% yield). ^{1}H NMR (300 MHz, $CDCl_3$): δ = 6.19 (br. s, 2 H, N*H*), 7.16 (m, 2 H, C*H*=CHCH=C*H*), 7.28 (m, 2 H, CH=C*H*C*H*=CH) ppm. ^{1}H NMR (300 MHz, C_6D_6): δ = 5.15 (br. s, 2 H, N*H*), 6.42 (m, 2 H, C*H*=CHCH=C*H*), 6.78 (m, 2 H, CH=C*H*C*H*=CH) ppm. ^{13}C{^{1}H} NMR (125 MHz, $CDCl_3$): δ = 122.9 (s, *C*H=CHCH=*C*H), 126.4

(s, CH=*C*H*C*H=CH), 132.0 (s, N_2C_2), 132.7 [dm, $^1J_{C,F}$ = 235 Hz, C_5F_4N], 144.1 (dm, $^1J_{C,F}$ = 240 Hz, C_5F_4N) ppm. ^{19}F NMR (282 MHz, $CDCl_3$): δ = –155.8 (m, 4 F, *o*-F), –92.1 (m, 4 F, *m*-F) ppm. ^{19}F NMR (282 MHz, C_6D_6): δ = –155.8 (m, 4 F, 3,5-F), –92.1 (m, 4 F, 2,6-F) ppm. MS (EI): *m*/*z* (%) = 406.1 (100) $[M]^+$, 367.1 (20) $[M – 2F]^+$, 236.1 (31) $[M – C_5F_4N – HF]^+$. $C_{16}H_6F_8N_4$ (406.23): calcd. C 47.31, H 1.49, N 13.79; found C 47.16, H 1.39, N 13.69.

***N*-(4′-Trimethylsilylphenyl)-3,6-di-*tert*-butylcarbazole (3):** A chilled solution (–78 °C, 2-propanol/liquid N_2 bath) of *N*-(4-bromophenyl)-3,6-di-*tert*-butylcarbazole (1.03 g, 2.4 mmol) in THF (20 mL) was combined with a solution of *tert*-butyllithium in *n*-pentane (3 mL, 4.8 mmol), and the 2-propanol/liquid N_2 bath was allowed to slowly warm to 0 °C. The mixture was recooled to –78 °C and a sample of chlorotrimethylsilane (0.32 g, 2.9 mmol) was added dropwise. The solution was warmed to room temperature before the addition of water (10 mL) and THF (30 mL). The organic layer was separated and washed with brine. The organic phase was dried with Na_2SO_4, and the solvent was removed in vacuo to afford pure **3** (0.98 g, 2.28 mmol, 95% yield) as a colorless solid. ^{1}H NMR (500 MHz, $CDCl_3$): δ = 0.38 [s, 9 H, Si(C*H*$_3$)$_3$], 1.49 (s, 18 H, *t*Bu), 7.41 (d, $^3J_{H,H}$ = 8.6 Hz, 2 H, *t*BuCCHC*H*C), 7.48 (dd, $^{3,4}J_{H,H}$ = 8.6, 1.7 Hz, 2 H, *t*BuCC*H*CHC), 7.57 (d, $^3J_{H,H}$ = 8.1 Hz, 2 H, NCCHCHCSi), 7.74 (d, $^3J_{H,H}$ = 8.1 Hz, 2 H, NCCHCHCSi), 8.16 (d, $^4J_{H,H}$ = 1.7 Hz, 2 H, *t*BuCC*H*C) ppm. ^{13}C{^{1}H} NMR (125 MHz, $CDCl_3$): δ = –0.8 [s, Si(*C*H$_3$)$_3$], 32.2 [s, C(*C*H$_3$)$_3$], 34.9 [*C*(CH$_3$)$_3$], 109.5 (s, *t*BuCCH*C*HC), 116.3 (s, *t*BuC*C*HC), 123.7 (s, *t*BuC*C*HCHC), 125.9 (s, NC*C*HCHCSi), 134.9 (s, NCCH*C*HCSi), 138.8 (s, NCCHCH*C*Si), 123.5,139.22, 142.9 (3s, *t*Bu*C*CH*CC*) ppm. MS (EI): *m*/*z* (%) = 427.3 (80) $[M]^+$, 412.2 (100) $[M – Me]^+$. $C_{29}H_{37}NSi$ (427.70): calcd. C 81.44, H 8.72, N 3.27; found C 81.69, H 9.07, N 3.25.

***N*-(5′-Trimethylsilylthien-2-yl)-3,6-di-*tert*-butylcarbazole (4):** A solution of *n*-butyllithium in *n*-hexane (6.7 mL, 10.7 mmol) was slowly added at room temperature to a well-stirred solution of *N*-(2′-thienyl)-3,6-di-*tert*-butylcarbazole (3.9 g, 10.7 mmol) in diethyl ether (100 mL). The mixture was stirred for 1 h at 20 °C before the addition of chlorotrimethylsilane (1.2 g, 11.0 mmol). After 16 h, water (50 mL) and diethyl ether (80 mL) were added. The organic layer was washed with brine and dried with Na_2SO_4. The solvent was removed in vacuo, and the residue was crystallized from ethanol to yield **4** (2.44 g, 5.9 mmol,55%) as pale yellow needles. ^{1}H NMR (500 MHz, $CDCl_3$): δ = 0.46 [s, 9 H, Si(C*H*$_3$)$_3$], 1.55 (s, 18 H, *t*Bu), 7.28 (d, $^3J_{H,H}$ = 3.5 Hz, 1 H, NCCHCHCS), 7.35 (d, $^3J_{H,H}$ = 3.5 Hz, 1 H, NCCHCHCS), 7.56 (m, 4 H, *t*BuCC*H*C*H*C), 8.20 (d, $^4J_{H,H}$ = 1.7 Hz, 2 H, *t*BuCC*H*C) ppm. ^{13}C{^{1}H} NMR (125 MHz, $CDCl_3$): δ = –0.04 [s, Si(*C*H$_3$)$_3$], 32.1 [s, C(*C*H$_3$)$_3$], 34.8 [s, *C*(CH$_3$)$_3$], 109.8 (s, *t*BuCCH*C*HC), 116.2 (s, *t*BuC*C*HC), 123.9 (s, *t*BuC*C*HCHC), 124.7 (s, NCCH*C*HCS), 133.0 (s, NC*C*HCHCS), 138.5 (s, NCCHCH*C*S), 123.5, 140.2, 143.5 (3s, *t*Bu*C*CH*CC*), 145.4 (s, N*C*CHCHCS) ppm. MS (EI): *m*/*z* (%) = 433.2 (100) $[M]^+$, 418.2 (95) $[M – Me]^+$. $C_{27}H_{35}NSSi$ (433.72): calcd. C 74.77, H 8.13, N 3.23; found C 74.47, H 8.16, N 3.33.

***N*-[4′-Dibromo(triphenylphosphonio)borato-phenyl]-3,6-di-*tert*-butylcarbazole (5):** A mixture of **3** (0.71 g, 1.64 mmol) and boron tribromide (0.43 g, 1.7 mmol) in CH_2Cl_2 (30 mL) was stirred for 16 h at room temperature. The solvent and volatile components were removed in vacuo, and the residue was redissolved in CH_2Cl_2 (30 mL). A solution of PPh_3 (0.446 g, 1.7 mmol) in CH_2Cl_2 (10 mL) was added to this mixture and stirring was continued for 2 h at room temperature. The solvent was removed to give crude **5** as a colorless solid, which was directly used for synthesis of **7**. ^{11}B{^{1}H}NMR (C_6D_6): δ = –4.8 ppm. ^{31}P NMR (C_6D_6): δ = –4.1 ppm.

***N*-[5′-Dibromo(triphenylphosphonio)borato-thien-2-yl]-3,6-di-*tert*-butylcarbazole (6):** Analogously, the mixture of **4** (0.71 g, 1.64 mmol) and BBr_3 (0.43 g, 1.7 mmol) in CH_2Cl_2 (30 mL) was stirred for 2 h at ambient temperature. The volatile compounds were removed in vacuo. The residue was dissolved in CH_2Cl_2 (30 mL), and a solution of PPh_3 (0.446 g, 1.7 mmol) in CH_2Cl_2 (10 mL) was added; stirring was continued for another 2 h. Crude **6** was obtained after removal of the solvent and was directly employed for further transformations. ^{11}B{^{1}H} NMR (C_6D_6): δ = 7.0 (bs) ppm. ^{31}P NMR (C_6D_6): δ = –4.2 ppm.

2-*N*-[4′-(3′′,6′′-Di-*tert*-butylcarbazolyl)phenyl]-1,3-bis(pentafluorophenyl)-1,3,2-benzodiazaborole (7): A slurry of **5** (1.291 g, 1.64 mmol) in toluene (30 mL) was combined with a solution of **1** (0.609 g, 1.5 mmol) in toluene (20 mL) and 2,2,6,6-tetramethylpiperidine (0.494 g, 3.5 mmol). The reaction mixture was stirred for 30 h at 100 °C. The mixture was cooled to ambient temperature and was filtered. The solvent and volatile components were removed from the filtrate in vacuo. Triphenylphosphane was separated from the residue by sublimation at 100 °C. Extraction of the residue with *n*-hexane afforded **7** (0.627 g, 0.78 mmol, 52% yield). ^{1}H NMR (500 MHz, $CDCl_3$): δ = 1.49 [s, 18 H, C(CH$_3$)$_3$], 6.91 (m, 2 H, C*H*=CHCH=C*H*), 7.20, (m, 2 H, CH=C*H*C*H*CH), 7.40 (d, $^3J_{H,H}$ = 9 Hz, NCCHCHCB), 7.47 (d, $^3J_{H,H}$ = 9 Hz, *t*BuCCHC*H*), 7.50 (dd, $^{3,4}J_{H,H}$ = 9, 2 Hz, *t*BuCC*H*CH) 7.54 (d, $^3J_{H,H}$ = 9 Hz, NCCHCHCB), 8.15 (d, $^4J_{H,H}$ = 2 Hz, *t*BuCC*H*C) ppm. ^{13}C{^{1}H} NMR (125 MHz, $CDCl_3$): δ = 31.9 [s, C(*C*H$_3$)$_3$], 34.7 [s, *C*(CH$_3$)$_3$], 109.2 (s, *C*H=CHCH=*C*H), 110.5 (s, *t*BuCCH*C*HC), 116.2 (s, *t*BuC*C*HC), 122.0 (s, CH=*C*H*C*H=CH), 123.7 (s, *t*BuC*C*HCHC), 126.1 (s, NCCHCHCB), 133.9 (s, NCCHCHCB), 135.9 (s, N_2C_2), 138.6 (s, N*C*CHCHCB), 123.6, 140.1, 143.3 (3s, *t*Bu*C*CH*CC*), 137.0 (dm, $^1J_{C,F}$ = 256 Hz, C_6F_5), 140.3 (dm, $^1J_{C,F}$ = 257 Hz, C_6F_5), 144 (dm, $^1J_{C,F}$ = 250 Hz, C_6F_5) ppm. ^{11}B{^{1}H} NMR (160 MHz, $CDCl_3$): δ = 30.7 ppm. ^{19}F NMR (470 MHz, $CDCl_3$): δ = –144.8 (m, 4 F, 2,6-F), –154.1 (t, $J_{F,F}$ = 24 Hz, 2 F, 4-F), –160.6 (m, 4 F, 3,5-F) ppm. MS (EI): *m*/*z* (%) = 803.3 (99) $[M]^+$, 788.3 (100) $[M – Me]^+$, 394.1 (20) $[BN_2C_6(C_6F_5)_2]^+$. $C_{44}H_{32}BF_{10}N_3$ (803.54): calcd. C 65.77, H 4.01, N 5.23; found C 65.68, H 3.91, N 5.13.

2[5′-(3′′,6′′-Di-*tert*-butylcarbazolyl)thien-2′-yl]-1,3-bis(pentafluorophenyl)-1,3,2-benzodiazaborole (8): Analogously to the preparation of **7**, a mixture of adduct **6** (1.301 g, 1.64 mmol), **1** (0.609 g, 1.5 mmol), and 2,2,6,6-tetramethylpiperidine (0.594 g, 3.50 mmol) in toluene (50 mL) was stirred for 16 h at 100 °C. The mixture was cooled to ambient temperature and filtered. The solvent was removed from the filtrate, and PPh_3 was removed from the solid residue by sublimation at 100 °C. The residue was triturated with *n*-hexane, and the filtered *n*-hexane solution was evaporated to dryness. A second sublimation at 120 °C was necessary to remove residual PPh_3. Product **8** was obtained as a pure colorless solid (0.546 g, 0.67 mmol, 45%). ^{1}H NMR (C_6D_6): δ = 1.34 [s, 18 H, C(CH$_3$)$_3$] 6.65 (m, 2 H, C*H*=CHCH=C*H*), 6.85 (d, $^3J_{H,H}$ = 4 Hz, 1 H, NCCHCHCS), 7.03 (d, $^3J_{H,H}$ = 4 Hz, 1 H, NCCHCHCS) 7.05 (m, 2 H, CH=CHCH=CH), 7.38 (s, 4 H, *t*BuCC*H*C*H*C) 8.20 (s, 2 H, *t*BuCC*H*C) ppm. ^{13}C{^{1}H} NMR (C_6D_6): δ = 31.6 [s, C(*C*H$_3$)$_3$], 34.4 [s, *C*(CH$_3$)$_3$], 109.7 (s, *C*H=CHCH=*C*H), 110.5 (s, *t*BuCCH*C*HC), 116.3 (s, *t*BuC*C*HC), 122.3 (s, CH=*C*H*C*H=CH), 124.2 (s, *t*BuC*C*HCHC), 124.5 (s, NCCHCHCS), 132.9 (s, NCCHCHCS), 136.1 (s, N_2C_2), 124.2, 139.9, 144.5 (3s, *t*Bu*C*CH*CC*), 137.0 (dm, $^1J_{C,F}$ = 255 Hz, C_6F_5), 140.5 (dm, $^1J_{C,F}$ = 254 Hz, C_6F_5), 144.5 (dm, $^1J_{C,F}$ = 252 Hz, C_6F_5), 146.6 (s, SCN)

ppm. $^{11}B\{^1H\}$ NMR (C_6D_6): δ = 27.7 ppm. ^{19}F NMR (C_6D_6): δ = –145.2 (m, 4 F, 2,6-F), –153.3 (t, 2 F, 4-F), 160.6 (m, 4 F, 3,5-F) ppm. MS (EI): *m*/*z* (%) = 809.3 (100) $[M]^+$, 794.3 (82) $[M – Me]^+$, 738.2 (12) $[M –2Me – 2HF]^+$. $C_{42}H_{30}BF_{10}N_3S$ (809.57): calcd. C 62.31, H 3.74, N 5.19; found C 60.63, H 4.06, N 4.89.

2-*N*-[4′-(3′′,6′′-Di-*tert*-butylcarbazolyl)phenyl]-1,3-bis(tetrafluoropyridyl)-1,3,2-benzodiazaborole (9): A mixture of **5** (1.291 g, 1.64 mmol), **2** (0.609 g, 1.50 mmol), and 2,2,6,6-tetramethylpiperidine (0.494 g, 3.5 mmol) in toluene (50 mL) was stirred for 48 h at 100 °C. After similar work-up, the colorless residue was continuously extracted with *n*-hexane over 16 h, whereby product **9** precipitated from the extract as a colorless solid (0.404 g, 0.53 mmol, 35%). ^1H NMR (500 MHz, C_6D_6): δ = 1.39 [s, 18 H, $C(CH_3)_3$], 6.55 (m, 2 H, C*H*=CHCH=C*H*), 7.01, (m, 4 H, CH=C*H*C*H*=CH and NCCHCHCB), 7.17 (d, $^3J_{H,H}$ = 4 Hz, 2 H, NCCHCHCB), 7.26 [d, $^3J_{H,H}$ = 8.6 Hz, *t*BuCCHC*H*], 7.35 (dd, $^3J_{H,H}$ = 8.6, 1.8 Hz, *t*BuCC*H*CH), 8.31 (d, $^4J_{H,H}$ = 1.8 Hz, *t*BuCC*H*C) ppm. $^{13}C\{^1H\}$ NMR (125 MHz, $CDCl_3$): δ = 30.0 [s, $C(CH_3)_3$], 34.7 [s, $C(CH_3)_3$], 109.8 (s, *C*H=CHCH=*C*H), 111.4 (s, *t*BuCCH*C*HC) 116.5 (s, *t*BuC*C*HC), 122.9 (s, CH=*C*H*C*H=CH), 124.0 (s, *t*BuC*C*HCHC), 125.7 (s, NCCHCHCB), 133.9 (s, NCCHCHCB), 135.4 (s, N_2C_2), 138.6 (dm, $^1J_{C,F}$ = 263 Hz, C_5F_4N), 144.3 (dm, $^1J_{C,F}$ = 240 Hz, C_5F_4N), 124.1, 139.6, 143.0 (3s, *t*Bu*C*CH*CC*) ppm. $^{11}B\{^1H\}$ NMR (160 MHz, C_6D_6): δ = 29.4 ppm. ^{19}F NMR (470 MHz, C_6D_6): δ = –87.7 (m, 4 F, 3,5-F), 145.1 (m, 4 F, 2,6-F) ppm. MS (EI): *m*/*z* (%) = 769.3 (89) $[M]^+$, 754.3 (100) $[M – Me]^+$, 698.2 (16) $[M –2Me – 2HF]^+$.

2-[5′-(3′′,6′′-Di-*tert*-butylcarbazolyl)thien-2′-yl]-1,3-bis(tetrafluoropyridyl)-1,3,2-benzodiazaborole (10): Prepared analogously to **9** from **6** (1.301 g, 1.64 mmol), **2** (0.609 g, 1.50 mmol), and 2,2,6,6-tetramethylpiperidine (0.494 g, 3.50 mmol) in toluene (50 mL) for 72 h at 100 °C, crude product **10** was obtained. The solid was removed in vacuo (1×10^{-6} bar), and the solid was extracted with *n*-pentane (2 × 40 mL). The combined extracts were stirred for 1 d in the presence of CuI (2 g). After filtration, the solution was concentrated to ca. 20 mL and stored at –20 °C. Within 2 d, product **10** separated as yellow crystals (0.200 g, 0.26 mmol, 16%). ^1H NMR (500 MHz, C_6D_6): δ = 1.34 [s, 18 H, $C(CH_3)_3$], 6.47 (m, 2 H, C*H*=CHCH=C*H*), 6.74 (d, $^3J_{H,H}$ = 4 Hz, 1 H, NCCHCHCS), 6.86 (d, $^3J_{H,H}$ = 4 Hz, 1 H, NCCHCHCS), 6.96 (m, 2 H, CH=C*H*C*H*=CH), 7.35 (d, $^3J_{H,H}$ = 8.7 Hz, 2 H, *t*BuCCHC*H*C), 7.42 (dd, $^{3,4}J_{H,H}$ = 8.7, 1.2 Hz, 2 H, *t*BuCC*H*CHC), 8.20 (s, $^3J_{H,H}$ = 1.2 Hz, 2 H, *t*BuCC*H*C) ppm. $^{13}C\{^1H\}$ NMR (125 MHz, C_6D_6): δ = 30.6 [s, $C(CH_3)_3$], 34.4 [s, $C(CH_3)_3$], 108.6 (s, *C*H=CHCH=*C*H), 110.0 (s, *t*BuCCH*C*HC), 115.3 (s, *t*BuC*C*HC), 121.9 (s, CH=*C*H*C*H=CH), 123.3 (s, *t*BuC*C*HCHC), 124.7 (s, NCCHCHCS), 133.9 (s, NCCHCHCS), 138.6 (dm, $^1J_{C,F}$ = 263 Hz, C_5F_4N), 144.0 (dm, $^1J_{C,F}$ = 231 Hz, C_5F_4N), 138.7 (s, N_2C_2), 123.5, 139.1, 143.2 (3s, *t*Bu*C*CH*CC*), 146.0 (s, S*C*N) ppm. $^{11}B\{^1H\}$ NMR (160 MHz, C_6D_6): δ = 28.9 ppm. ^{19}F NMR (282 MHz, C_6D_6): δ = –87.4 (m, 4 F, 3,5-F), –144.7 (m, 4 F, 2,6-F) ppm. MS (EI): *m*/*z* (%) = 775.5 (100) $[M]^+$, 760.5 (94) $[M – Me]^+$.

2-*N*-[4′-(3′′,6′′-Di-*tert*-butylcarbazolyl)phenyl]-1,3-diphenyl-1,3,2-benzodiazaborole (11): A chilled solution (–78 °C) of *N*-(4-bromophenyl)-3,6-di-*tert*-butylcarbazole (1.00 g, 2.30 mmol) in diethyl ether (50 mL) was treated with an equimolar amount of *n*-butyllithium dissolved in *n*-hexane (1.6 M, 1.44 mL, 2.3 mmol). The reaction mixture was warmed to 0 °C, and was then recooled to –78 °C before a solution of 2-bromo-1,3-diphenyl-1,3,2-benzodiazaborole (0.91 g, 2.3 mmol) in benzene (15 mL) was added. The mixture was stirred for 16 h at ambient temperature, and the solvent and volatile components were removed in vacuo. The obtained solid residue was continuously extracted with *n*-hexane over 2 d, whereupon product **11** separated as a colorless solid (0.90 g, 1.44 mmol, 63%). ^1H NMR (500 MHz, $CDCl_3$): δ = 1.50 (s, 18 H, *t*Bu), 7.10 (m, 2 H, C*H*=CHCH=C*H*), 7.16 (m, 2 H, CH=C*H*C*H*=CH), 7.36 (m, 6 H, *t*BuCCHC*H*, NCC*H*C*H*CB), 7.46 (m, 8 H, BNPh, *m*-H Ph, *p*-H Ph and *t*BuCC*H*CH), 7.53 (m, 4 H, BNPh, *o*-Ph), 8.15 (d, $^4J_{H,H}$ = 1.7 Hz, 2 H, *t*BuCC*H*C) ppm. $^{13}C\{^1H\}$ NMR (125 MHz, $CDCl_3$): δ = 32.0 [s, $C(CH_3)_3$], 34.7 [s, $C(CH_3)_3$], 109.4 (s, *C*H=CHCH=*C*H), 110.2 (s, *t*BuCCH*C*H), 116.1 (s, *t*BuC*C*HC), 120.1 (s, CH=*C*H*C*H=CH), 123.4 (s, *t*BuC*C*HCH), 125.2 (s, NCCHCHCB), 126.6 (s, NCCH=CH*C*H), 127.9, 129.4 (2s, NC*C*H=*C*HCH), 136.1 (s, NCCHCHCB), 123.5, 140.4, 142.9 (3s, C-carbazole), 137.9 (s, BN*C*-CHCHCH), 138.5 (s, N*C*CHCHCB), 138.8 (s, N_2C_2), 144.5 (s, S*C*N) ppm. $^{11}B\{^1H\}$ NMR (160 MHz, $CDCl_3$): δ = 29.2 ppm. MS (EI): *m*/*z* (%) = 623.4 (100) $[M]^+$, 608.2 (64) $[M – CH_3]^+$. $C_{44}H_{42}BN_3$ (623.64): calcd. C 84.74, H 6.79, N 6.74; found C 84.18, H 7.17, N 6.71.

Further details of the crystallographic data for **8** are given in Table 7. CCDC-925364 contains the supplementary crystallographic data for this paper. These data can be obtained free of charge from The Cambridge Crystallographic Data Centre via www.ccdc.cam.ac.uk/data_request/cif.

Table 7. Crystallographic data for **8**.

Empirical formula	$C_{42}H_{30}BF_{10}N_3S$
M_r [g mol^{-1}]	809.56
Crystal dimensions [mm]	0.08 × 0.07 × 0.06
Crystal system	monoclinic
Space group	$P\ 2_1/c$
a [Å]	12.9805(4)
b [Å]	23.2787(10)
c [Å]	12.7744(5)
β [°]	98.854(2)
V [Å^3]	3814.0(3)
Z	4
$\rho_{calcd.}$ [g cm^{-3}]	1.410
μ [mm^{-1}]	0.169
F (000)	1656
Θ [°]	3–25
Reflections collected	44982
Unique reflections	6692
R(int)	0.113
Reflections [$I > 2\sigma(I)$]	4014
Refined parameters	520
GOF	1.009
R_F [$I > 2\sigma(I)$]	0.0520
wR_{F2} (all data)	0.1230
$\Delta\rho_{max/min}$ [e Å^{-3}]	0.242/–0.240

Supporting Information (see footnote on the first page of this article): Tables of atomic coordinates for [CAM-B3LYP/6-311G(d,p)] optimized geometries, values of total energies and Lippert–Mataga plots of **7**–**10**.

[1] a) C. D. Entwistle, T. B. Marder, *Angew. Chem.* **2002**, *114*, 3051–3056; *Angew. Chem. Int. Ed.* **2002**, *41*, 2927–2931; b) Y. Shirota, *J. Mater. Chem.* **2000**, *10*, 1–25; c) S. Yamaguchi, A. Wakayama, *Pure Appl. Chem.* **2006**, *78*, 1413–1424; d) F. Jäkle, *Coord. Chem. Rev.* **2006**, *250*, 1107–1121; e) F. Jäkle, *Chem. Rev.* **2010**, *110*, 3985–4022; f) M. Elbing, G. C. Bazan, *Angew. Chem.* **2008**, *120*, 846–850; *Angew. Chem. Int. Ed.* **2008**, *47*, 834–838; g) T. W. Hudnall, C.-W. Chiu, F. P. Gabbai, *Acc. Chem. Res.* **2009**, *42*, 388–397; h) N. Matsumi, Y. Chujo, *Polym. J.* **2007**, *40*, 77–89; i) Z. M. Hudson, S. Wang, *Acc. Chem.*

Res. **2009**, *42*, 1584–1596; j) C. D. Entwistle, T. B. Marder, *Chem. Mater.* **2004**, *16*, 4574–4585.

[2] a) M. E. Glogowski, J. L. R. Williams, *J. Organomet. Chem.* **1981**, *218*, 137–146; b) A. Sundararaman, R. Varughese, H. Li, L. N. Zakharov, A. L. Rheingold, F. Jäkle, *Organometallics* **2007**, *26*, 6126–6131.

[3] A. Schulz, W. Kaim, *Chem. Ber.* **1989**, *122*, 1863–1868.

[4] a) C.-H. Zhao, A. Wakamiya, Y. Inukai, S. Yamaguchi, *J. Am. Chem. Soc.* **2006**, *128*, 15934–15935; b) H. Li, A. Sundararaman, K. Venkatasubbaiah, F. Jäkle, *J. Am. Chem. Soc.* **2007**, *129*, 5792–5793; c) A. Wakamiya, K. Mori, S. Yamaguchi, *Angew. Chem.* **2007**, *119*, 4351–4354; *Angew. Chem. Int. Ed.* **2007**, *46*, 4273–4276.

[5] a) L. Weber, *Coord. Chem. Rev.* **2001**, *215*, 39–77; b) L. Weber, *Coord. Chem. Rev.* **2008**, *252*, 1–31; c) L. Weber, *Eur. J. Inorg. Chem.* **2012**, 5595–5609; d) M. Yamashita, K. Nozaki, *J. Synth. Org. Chem. Jpn.* **2010**, *68*, 359–369; e) M. Yamashita, K. Nozaki, *Pure Appl. Chem.* **2008**, *80*, 1187–1194; f) M. Yamashita, K. Nozaki, *Bull. Chem. Soc. Jpn.* **2008**, *81*, 1377–1392; g) L. Weber, H. B. Wartig, H.-G. Stammler, B. Neumann, *Organometallics* **2001**, *20*, 5248–5250; h) L. Weber, H. B. Wartig, H. G. Stammler, B. Neumann, *Z. Anorg. Allg. Chem.* **2001**, *627*, 2663–2668; i) L. Weber, I. Domke, W. Greschner, K. Miqueu, A. Chrostowska, P. Baylère, *Organometallics* **2005**, *24*, 5455–5463.

[6] a) T. Habereder, H. Nöth, *Appl. Organomet. Chem.* **2003**, *17*, 525–538; b) L. Weber, I. Domke, J. Kahlert, H.-G. Stammler, *Eur. J. Inorg. Chem.* **2006**, 3419–3424; c) L. Weber, A. Rausch, H. G. Stammler, B. Neumann, *Z. Anorg. Allg. Chem.* **2004**, *630*, 2657–2664; d) L. Weber, J. Förster, H.-G. Stammler, B. Neumann, *Eur. J. Inorg. Chem.* **2006**, 5048–5056; e) L. Weber, M. Schnieder, T. C. Maciel, H. B. Wartig, M. Schimmel, R. Boese, D. Bläser, *Organometallics* **2000**, *19*, 5791–5794; f) J. M. Murphy, J. D. Lawrence, K. Kawamura, C. Incarvito, J. F. Hartwig, *J. Am. Chem. Soc.* **2006**, *128*, 13684–13685; g) Y. Segawa, M. Yamashita, K. Nozaki, *Science* **2006**, *314*, 113–115; h) T. B. Marder, *Science* **2006**, *314*, 69–70; i) H. Braunschweig, *Angew. Chem.* **2007**, *119*, 1990–1992; *Angew. Chem. Int. Ed.* **2007**, *46*, 1946–1948; j) Y. Segawa, M. Yamashita, K. Nozaki, *Angew. Chem.* **2007**, *119*, 6830–6833; *Angew. Chem. Int. Ed.* **2007**, *46*, 6710–6713; k) T. Kajiwara, T. Terabayashi, M. Yamashita, K. Nozaki, *Angew. Chem.* **2008**, *120*, 6708–6712; *Angew. Chem. Int. Ed.* **2008**, *47*, 6606–6610; l) Y. Segawa, Y. Suzuki, M. Yamashita, K. Nozaki, *J. Am. Chem. Soc.* **2008**, *130*, 16069–16079; m) M. Yamashita, Y. Suzuki, Y. Segawa, K. Nozaki, *Chem. Lett.* **2008**, *37*, 802–803; n) T. Terabayashi, T. Kajiwara, M. Yamashita, K. Nozaki, *J. Am. Chem. Soc.* **2009**, *131*, 14162–14163; o) K. Nozaki, Y. Arami, M. Yamashita, S.-H. Ueng, M. Malacria, E. Lacôte, D. P. Curran, *J. Am. Chem. Soc.* **2010**, *132*, 11449–11451; p) Y. Hayashi, Y. Segawa, M. Yamashita, K. Nozaki, *Chem. Commun.* **2011**, *47*, 5888–5890; q) Y. Segawa, M. Yamashita, K. Nozaki, *Organometallics* **2009**, *28*, 6234–6242; r) M. Hasegawa, Y. Segawa, M. Yamashita, K. Nozaki, *Angew. Chem.* **2012**, *124*, 7062–7066; *Angew. Chem. Int. Ed.* **2012**, *51*, 6956–6960; s) N. Dettenrieder, H. M. Dietrich, C. Schädle, C. Maichle-Mössmer, K. W. Törnroos, R. Anwander, *Angew. Chem.* **2012**, *124*, 4537–4541; *Angew. Chem. Int. Ed.* **2012**, *51*, 4461–4465; t) A. V. Protchenko, K. H. Birjkumar, D. Dange, A. D. Schwarz, D. Vidovic, C. Jones, N. Kaltsoyannis, P. Mountford, S. Aldridge, *J. Am. Chem. Soc.* **2012**, *134*, 6500–6503; u) L. M. A. Saleh, K. H. Birjkumar, A. V. Protchenko, A. D. Schwarz, S. Aldridge, C. Jones, N. Kaltsoyannis, P. Mountford, *J. Am. Chem. Soc.* **2011**, *133*, 3836–3839; v) S. Li, J. Cheng, Y. Chen, M. Nishiura, Z. Hou, *Angew. Chem.* **2011**, *123*, 6484–6487; *Angew. Chem. Int. Ed.* **2011**, *50*, 6360–6363; w) D. Tian, J. Jiang, H. Hu, J. Zhang, C. Cui, *J. Am. Chem. Soc.* **2012**, *134*, 14666–14669; x) A. Hinchliffe, F. S. Mair, E. J. L. McInnes, R. G. Pritchard, J. E. Warren, *Dalton Trans.* **2008**, 222–233; y) E. Giziroglu, B. Donnadieu, G. Bertrand, *Inorg. Chem.* **2008**, *47*, 9751–9753.

[7] a) A. Chrostowska, M. Maciejczyk, A. Dargelos, P. Baylère, L. Weber, V. Werner, D. Eickhoff, H.-G. Stammler, B. Neumann, *Organometallics* **2010**, *29*, 5192–5198; b) L. Weber, J. Halama, V. Werner, K. Hanke, L. Böhling, A. Chrostowska, A. Dargelos, M. Maciejczyk, A.-L. Raza, H.-G. Stammler, B. Neumann, *Eur. J. Inorg. Chem.* **2010**, 5416–5425; c) S. Maruyama, Y. Kawanishi, *J. Mater. Chem.* **2002**, *12*, 2245–2249; d) L. Weber, I. Domke, C. Schmidt, T. Braun, H.-G. Stammler, B. Neumann, *Dalton Trans.* **2006**, 2127–2132; e) L. Weber, A. Penner, I. Domke, H. G. Stammler, B. Neumann, *Z. Anorg. Allg. Chem.* **2007**, *633*, 563–569; f) L. Weber, D. Eickhoff, V. Werner, L. Böhling, S. Schwedler, A. Chrostowska, A. Dargelos, M. Maciejczyk, H.-G. Stammler, B. Neumann, *Dalton Trans.* **2011**, *40*, 4434–4446; g) S. Schwedler, D. Eickhoff, R. Brockhinke, D. Cherian, L. Weber, A. Brockhinke, *Phys. Chem. Chem. Phys.* **2011**, *13*, 9301–9310; h) L. Weber, V. Werner, I. Domke, H.-G. Stammler, B. Neumann, *Dalton Trans.* **2006**, 3777–3784; i) L. Weber, V. Werner, M. A. Fox, T. B. Marder, S. Schwedler, A. Brockhinke, H.-G. Stammler, B. Neumann, *Dalton Trans.* **2009**, 2823–2831.

[8] L. Weber, D. Eickhoff, T. B. Marder, M. A. Fox, P. J. Low, A. D. Dwyer, D. J. Tozer, S. Schwedler, A. Brockhinke, H.-G. Stammler, B. Neumann, *Chem. Eur. J.* **2012**, *18*, 1369–1382.

[9] L. Weber, H. Kuhtz, L. Böhling, A. Brockhinke, A. Chrostowska, A. Dargelos, A. Maziere, H.-G. Stammler, B. Neumann, *Dalton Trans.* **2012**, *41*, 10440–10452.

[10] L. Weber, J. Kahlert, R. Brockhinke, L. Böhling, A. Brockhinke, H.-G. Stammler, B. Neumann, R. A. Harder, M. A. Fox, *Chem. Eur. J.* **2012**, *18*, 8347–8357.

[11] L. Weber, V. Werner, M. A. Fox, T. B. Marder, S. Schwedler, A. Brockhinke, H.-G. Stammler, B. Neumann, *Dalton Trans.* **2009**, 1339–1351.

[12] M. M. Khusniyarov, K. Harms, O. Burghaus, J. Sundermeyer, B. Sarkar, W. Kaim, J. van Slageren, C. Duboc, J. Fiedler, *Dalton Trans.* **2008**, 1355–1365.

[13] E. Lippert, *Z. Elektrochem.* **1957**, *61*, 962–975.

[14] a) A. Hameurlaine, W. Dahaen, *Tetrahedron* **2003**, *44*, 957–959; b) M. Herm, *PhD. Thesis*, Martin-Luther-Universität Halle-Wittenberg, **2003**.

[15] M. J. Frisch, G. W. Trucks, H. B. Schlegel, G. E. Scuseria, M. A. Robb, J. R. Cheeseman, G. Scalmani, V. Barone, B. Mennucci, G. A. Petersson, H. Nakatsuji, M. Caricato, X. Li, H. P. Hratchian, A. F. Izmaylov, J. Bloino, G. Zheng, J. L. Sonnenberg, M. Hada, M. Ehara, K. Toyota, R. Fukuda, J. Hasegawa, M. Ishida, T. Nakajima, Y. Honda, O. Kitao, H. Nakai, T. Vreven, J. A. Montgomery Jr., J. E. Petralta, F. Ogliaro, M. Bearpark, J. J. Heyd, E. Brothers, K. N. Kudin, V. N. Staroverov, R. Kobayashi, J. Normand, K. Raghavachari, A. Rendell, J. C. Burant, S. S. Iyengar, J. Tomasi, M. Cossi, N. Rega, J. M. Millam, M. Klene, J. E. Knox, J. B. Cross, V. Bakken, C. Adamo, J. Jaramillo, R. Gomperts, R. E. Stratmann, O. Yazyev, A. J. Austin, R. Cammi, C. Pomelli, J. W. Ochterski, R. L. Martin, K. Morokuma, V. G. Zakrzewski, G. A. Voth, P. Salvador, J. J. Dannenberg, S. Dapprich, A. D. Daniels, Ö. Farkas, J. B. Foresman, J. V. Ortiz, J. Cioslowski, D. J. Fox, *Gaussian 09*, revision A.02, Gaussian, Inc. Wallingford CT, **2009**.

[16] a) R. G. Parr, W. Yang, *Functional Theory of Atoms and Molecules*, Oxford University Press, New York, **1989**; b) M. J. Frisch, G. W. Trucks, J. R. Cheeseman, in: *Recent Development and Applications of Modern Density Functional Theory, Theoretical and Computational Chemistry* (Ed.: J. M. Semminario), Elsevier, Amsterdam, **1996**, vol. 4, p. 679–707.

[17] T. Yanai, D. Tew, N. Handy, *Chem. Phys. Lett.* **2004**, *393*, 51.

[18] a) R. E. Stratmann, G. E. Scuseria, M. J. Frisch, *J. Chem. Phys.* **1998**, *109*, 8218; b) M. E. Casida, C. Jamorski, K. C. Casida, D. R. Salahub, *J. Chem. Phys.* **1998**, *108*, 4439; c) V. Lemierre, A. Chrostowska, A. Dargelos, H. Chermette, *J. Phys. Chem. A* **2005**, *109*, 8348.

Received: March 8, 2013
Published Online: ■

